Surface & Coatings Technology 205 (2011) 3218–3225

Contents lists available at ScienceDirect

Surface & Coatings Technology

journal homepage: www.elsevier.com/locate/surfcoat

Effect of heat-treatment on stress relaxation behavior of plasma-sprayed 7 wt.% Y_2O_3–ZrO_2 stand-alone coatings

Christopher Petorak, Rodney W. Trice *

Purdue University, School of Materials Engineering, West Lafayette, IN 47907, USA

ARTICLE INFO

Article history:
Received 30 July 2010
Accepted in revised form 16 November 2010
Available online 25 November 2010

Keywords:
Thermal barrier coatings
YSZ
Mechanical properties
Stress relaxation

ABSTRACT

The present work studied the effect of heat-treatment temperature (1000 °C and 1200 °C) and time (10, 50, and 100 h) on the compressive stress relaxation behavior of plasma-sprayed stand-alone 7 wt.% Y_2O_3–ZrO_2 (YSZ) coatings at test temperatures of 1000 °C, 1100 °C, and 1200 °C, from stresses of 60 and 20 MPa. As-sprayed coatings were also stress relaxed in the baseline condition at room and elevated temperatures. All coatings demonstrated a two-stage relaxation behavior: fast relaxation (stage I) in the first 10 min and much slower relaxation in the final 170 min of the test (stage II). Stage I relaxation, as measured by percentage of the original stress relaxed, accounts for at least 50% of the total stress relaxed despite occurring in only 5–10 min and was attributed to lamella sliding and compaction, and permanent intralamellar crack closure (for tests conducted at higher temperatures). Stage II relaxation behavior is dominated by diffusion creep mechanisms, where prior densification at 1200 °C resulted in reduced relaxation rates compared to coatings heat treated at 1000 °C and in the as-sprayed condition. The 1200 °C test temperature greatly influenced the percentage of relaxation in the coating, more so than the prior coating heat-treatment conditions.

1. Introduction

The efficiency of a gas turbine engine is dictated by the maximum operating temperature during operation. Application of a thin insulating ceramic coating, i.e. a thermal barrier coating (TBC), to the hot sections of the engine afford higher operating temperatures, resulting in increased efficiency [1–4]. The ceramic topcoat, usually a 7 wt.% yttria-stabilized zirconia (YSZ), typically ranges in thickness from ~120 to ~250 μm in turbine applications [1–4].

Service conditions place the coating in a biaxial compressive stress state during heat-up and a biaxial tensile stress state upon cool down [5,6]. The compressive stress, which is highest in magnitude at the free surface, is relaxed with time in air plasma-sprayed (APS) coatings by a combination of mechanisms including sintering, compaction, and time-dependent mechanical deformation [7–10]. A significant fraction of the stress relaxation behavior in APS YSZ coatings is tied to the characteristic microstructure associated with the APS process which includes cracks that cut lamella (i.e. intralamellar cracks) and pores between lamella (i.e. interlamellar pores); the other fraction is tied to the intrinsic properties of the YSZ [9–11]. Interestingly, the microstructural changes that assist compressive relaxation at high temperature correspondingly limit recovery during cooling.

The inability of the APS coating to recover to its original dimensions during cooling causes in-plane biaxial tension in the coating. When the tensile stresses exceed the fracture strength of the newly sintered and compacted YSZ, the energy is relieved by through-thickness crack growth and possible delamination of the coating at the interface [12–14]. Therefore, an understanding of compressive stress relaxation in APS coatings, which is proportionally linked to the magnitude of tensile stress that develop in the coatings upon cooling, provides the key step in microstructural design for future coatings, specifically by isolating relaxation mechanisms that prevent recovery.

Relaxation has been previously studied in the as-sprayed condition for YSZ coatings [7–10,15]. But it is well documented that exposure to high temperature results in morphological changes in the APS microstructure, specifically formation of sintering necks, spheroidization or healing of fine cracks, redistribution of pores and transformation of the system of lamella splats from a primarily mechanically interlocked to a chemically bonded one. Typically, heat-treated APS coatings display increased modulus and fracture strengths compared to as-sprayed coatings [16–21]. The temperature plays a role in the mass transport mechanism, and therefore, the nature of the microstructural changes that occur. Surface diffusion of atoms has been observed in YSZ at 1000 °C and will lead to microstructural coarsening but not densification of the coating. At 1200 °C, coating densification occurs via bulk transport of atoms [22].

The purpose of our present work is to study the effect of heat-treatment on the time-dependent mechanical behavior of stand-alone YSZ coatings at elevated temperatures. APS YSZ samples were heat treated at 1000 °C and 1200 °C for 50 h to differentiate between the

* Corresponding author. Tel.: +1 765 494 6405.
E-mail address: rtrice@purdue.edu (R.W. Trice).

0257-8972/$ – see front matter © 2010 Elsevier B.V. All rights reserved.
doi:10.1016/j.surfcoat.2010.11.040

effects of microstructural coarsening and microstructure sintering, respectively. Heat-treatment times of 10 and 100 h at 1200 °C were used to distinguish the effects of sintering duration.

2. Experimental procedure

2.1. Sample fabrication and physical testing

Cylindrical stand-alone coatings were produced from a 7 wt.% Y_2O_3–93 wt.% ZrO_2 powder[1] having a particle size of 22.5 ± 6.0 μm. The coatings were sprayed at Ames National Laboratory using a Praxair SG-100 gun. The spray parameters are listed in Table 1. Coatings were fabricated by rastering the plasma gun up and down the rotating copper rod, which were then sectioned into sample lengths between 15 and 18 mm by lathe using a diamond cutting tool. The copper substrate was etched from the YSZ coating with nitric acid to leave the stand-alone coating.

Several stand-alone coatings were then subjected to heat treatments of 10, 50 and 100 h at 1200 °C, and 50 h at 1000 °C, while leaving a number of coatings in the as-sprayed condition as a control group to compare to the heat-treated samples. Heat-treatment temperatures of 1000 °C and 1200 °C where utilized to differentiate the effects of microstructural coarsening versus microstructural densification of plasma-sprayed YSZ coatings [22–24].

The Archimedes method was used to determine the bulk density and total porosities of the coatings in the as-sprayed condition and then again in the heat-treated conditions, assuming 6.08 g/cm^3 as the theoretical density of 7 wt.% YSZ [25].

2.2. Stress relaxation

The test rig and methods employed in the current research were previously described in detail by Dickinson et al. [10]. and are only highlighted here. High temperature compression testing was performed using a servo-hydraulic load frame[2] equipped with hydraulic collet grips, an alignment fixture,[3] a 100 kN force transducer, SiC pushrods, and a high temperature furnace.[4] Strain was measured with a high temperature extensometer[5] with a resolution of ±1 μm. Strain was measured as the extensometer recorded any displacement between the stationary upper compression platen and the cantilever supporting the pushrod. Alignment of the load frame was adjusted prior to testing the coatings to ensure that load was distributed equally around the circumference of the sample.

Stress relaxation test temperatures for heat-treated coatings were 1100 °C and 1200 °C. In addition, as-sprayed coatings samples were stress relaxed at 25 °C and 1000 °C. Stress relaxation experiments were performed on as-sprayed coatings at room temperature to quantify time-dependent behavior for comparison with stress relaxation experiments conducted at elevated temperatures. These experiments afford differentiation of deformation mechanisms occurring at room temperature from those occurring due to the elevated test temperature. The initial applied compressive stress of either 20 or 60 MPa was monotonically applied at a rate of 20 N/s. At the instant the desired stress was attained, the control mode switched from a load feedback loop using the force transducer, to a constant displacement feedback loop using the extensometer. The system was maintained under strain control for 180 min at the desired test temperature. It should be noted that no load was applied until the furnace had soaked at the desired temperature for 15 min. The noise in the load signal represents ±1 MPa uncertainty.

[1] H.C.-Starck, Amperit 825.0.
[2] MTS 810 Load Frame.
[3] MTS 609 Alignment Fixture.
[4] Applied Test Systems, Inc. High Temperature Furnace.
[5] MTS 632.70H-01.

Table 1
Spray parameters of coatings.

Spray Parameter	value
Power (kW)	37
Stand-off distance (cm)	10
Arc gas rate (slm)	25 (Ar)
Aux gas rate (slm)	21 (He)
Powder carrier gas rate (slm)	6 (Ar)
Powder feed rate (rpm)	1.5

2.3. Stress relaxation modeling

A Maxwell element, consisting of an elastic spring and viscous dashpot in series, is often used to model the stress relaxation behavior of polymeric materials [26–29]. A modified two element Maxwell model is utilized in the current study to characterize the relaxation behavior for APS coatings. The model consisted of two Maxwell elements in parallel with an additional spring element. The 2-element Maxwell model is analogous to mathematically adding two separate stress relaxation behaviors (fast and slow relaxation) at each time increment, yielding one stress relaxation curve.

Differentiation between regimes, and the physical processes dominating the relaxation behavior within these regimes, was characterized through the assignment of τ_1 and w_1, and τ_2 and w_2. The solution to the modified two-element Maxwell model plus spring is given by:

$$\sigma(t) = \sigma_o \sum_{k=1}^{n} \frac{w_k}{100} \exp\left(-\frac{t}{\tau_k}\right) + \frac{w_3}{100}\sigma_o \tag{1}$$

where σ_o is the initial stress, n is 2 (i.e. the number of Maxwell elements in parallel), $w_k$is the percentage of σ_o relaxed, and t is time. After the 180 min test the percentage residual stress remaining in the coating, if any, is given by w_3 which is defined as:

$$w_3 = 100 - (w_1 + w_2). \tag{2}$$

The time constant for each Maxwell element, τ_k, can be further defined as:

$$\tau_k = \frac{\eta_k}{E_k}. \tag{3}$$

where η_k is the viscosity of the dashpot and E_k is the modulus of the spring for each Maxwell element. Due to the exponential form of Eq. (1), $5\tau_1$ represents 99.4% relaxation of Maxwell element 1 (fast relaxation), and $5\tau_2$ represents the same percentage of relaxation for Maxwell element 2 (slow relaxation). Mathematically, complete relaxation of the 2 Maxwell element model is given in seconds by $5\tau_1 + 5\tau_2$. Experimentally, though, complete relaxation occurs when the stress in the coating is relaxed to 1 MPa based on the experimental uncertainties established.

Individual τ_k and w_k were fit to a given set of experimental data using a least-squares curve fitting method by minimizing R as defined in the following equation:

$$R = \sum_{t=0}^{t=t_f} \sqrt{\left|\left[\sigma_{\exp}(t)\right]^2 - \left[\sigma_{\mathrm{mod}}(t)\right]^2\right|} \tag{4}$$

where $\sigma_{\exp}(t)$ and $\sigma_{\mathrm{mod}}(t)$ represent stress values obtained experimentally and from numerical modeling, respectively, from the start of the test ($t=0$) until the end of the test ($t=t_f$). The R value has no physical meaning, but is minimized to provide the best fit of the model to the experimental data. Stress values were squared to give higher stress values greater weight in determining a proper fit. The square root of this difference for each time-step is summed over the

complete test time, yielding an R value. This value can be minimized by iteratively varying τ_k and w_k and thereby providing the best fit of the model to the experimental stress relaxation data.

2.4. Stress relaxation data processing

Strain rates were extracted from modeled stress relaxation data using a method described previously [30,31] and the highlights are only presented here. The constant applied strain in a stress relaxation experiment is achieved by maintaining a constant displacement between the upper and lower platens, which is measured and maintained by the extensometer. The initially applied uniaxial strain is stored as elastic energy in the sample, which with time can be dissipated through permanent deformation. Because the load frame is in static equilibrium, there must be an equal and opposite elastic energy stored in the load frame. Assuming purely elastic displacements in the load frame during loading, the non-elastic strain in the sample can be determined.

The force at a given instant during relaxation provides a link to the displacement of the load frame as a function of the applied load. Strain rates can be extracted from the stress relaxation data by using the known displacement of the load frame as a function of applied load at a given temperature, and the applied load at a given instant in time. Thus, a compliance curve was measured for the load frame that related the force, designated P, and the elastic displacement of the load frame, designated Δ. Therefore, the function $\Delta(P)$ expresses the displacement of the load frame for any applied force. Secondly, $P(t)$ for each coating condition at a given temperature was established. The length, or dimension along the uniaxially applied stress direction, of the coating can be expressed as a function of time by relating $\Delta(P)$ and $P(t)$.

The instantaneous length of the sample, $l(t)$, is then simply the initial length of the sample, l_o, minus the length of the sample due to the initially applied load at the onset of testing, L_o, and the displacement of the load cell as a function of time, $\Delta(P(t))$. Note that Δh_{sample} is the change in height of the sample. The instantaneous length of the sample, $l(t)$ is then:

$$l(t) = l_o - \left(\Delta h_{sample}\right) = l_o - (L_o - \Delta(P(t))) = l_o - L_o + \Delta(P(t)) \quad (5)$$

where, L_o is the displacement of the cross-head according to the extensometer at the onset of stress relaxation when $t = 0$ s. The strain rate at a given instant during stress relaxation is given by

$$\dot{\varepsilon} = \varepsilon(t) = -\frac{1}{l(t)}\frac{d}{dt}l(t) \quad (6)$$

The physical limitation of the equipment used to measure the stress relaxation behavior provides an uncertainty for measuring changes in strain of ± 0.00007 that can be sampled every 0.0002 s, which provides the limitation for measuring the strain rate to be 1.4×10^{-8} 1/s.

The loading curves prior to stress relaxation were used to establish the modulus for a given coating condition at elevated temperatures. The compliance of the load frame was measured and removed from data sets to establish the compressive modulus of the coating.

3. Results and discussion

3.1. Effects of heat-treatment on physical properties of APS YSZ coatings

A more complete microstructural analysis of coatings prepared using identical processing parameters and the same starting powder was published previously [32] and the results are highlighted here. In brief, SEM micrographs revealed a typical plasma-sprayed microstructure made up of stacked lamella. From small angle neutron scattering (SANS) data it was observed that interlamellar pores were oriented perpendicular to the spray direction and intralamellar cracks parallel to the spray direction. With respect to the cylindrical geometry of the specimen, some of the cracks were oriented such that the uniaxially applied stress would act to close them. The stand-alone coatings had an average height of 16.07 ± 1.35 mm, an outer diameter of 13.80 ± 0.04 mm, and a thickness of 0.56 ± 0.02 mm in the as-sprayed condition. Changes in the coatings height, thickness and outer diameter due to heat-treatment were not statistically differentiated by caliper measurement. For example, the average of 14 coatings heat treated for either 10 h or 50 h at 1200 °C demonstrated changes in height of 0.03 ± 0.02 mm and 0.06 ± 0.03 mm, respectively. Thus, there is an overlap of the first standard deviations of coating height changes for both heat-treatment times.

Archimedes tests comparing the as-sprayed and heat-treated coatings exhibited no statistical difference in the density for established measurement errors of ± 0.14 g/cm^3. For example, the density of as-sprayed, 10 h/1200 °C, and 100 h/1200 °C heat-treated coatings was 5.52 g/cm^3, 5.55 g/cm^3, and 5.60 g/cm^3, respectively [37]. The largest contributor to measurement error is the small mass of the samples, generally <1 g. However, SANS results indicated that a 3-hr heat-treatment at 1200 °C (shorter than the 50-hr heat treatments used in the present study) on identically prepared coatings tended to reduce the amount of surface area associated with the cracks and pores [32]. This is consistent with other studies [33–35] and direct observation of microstructures after heat treatments [22].

Table 2 shows that the affect of heat-treatment and test temperature on elastic modulus. As-sprayed coatings tested at 1000 °C, 1100 °C, and 1200 °C demonstrated an initial loading modulus of 19, 14, and 15 GPa. However, it must be remembered that the coatings were stabilized for 15 min at the test temperature prior to loading and therefore the modulus values are not on "as-sprayed" coatings, per se. Also, it is difficult to deconvolute the effect of sintering (which would be expected to increase modulus) from the fact that the modulus of most materials generally decreases with temperature increase. However, it was generally noted that the strain necessary to achieve 60 MPa decreased with heat-treatment, a consequence of the increase in elastic modulus with heat-treatment. For example, at the test temperature of 1200 °C and the initial strain to achieve 60 MPa decreased from 0.0046 to 0.0028 for the as-sprayed and 50 h/1200 °C heat-treated samples, respectively.

3.2. Overview of stress relaxation behavior of APS YSZ

Representative stress relaxation curves are shown in Fig. 1a, b, and c; independent of testing variables all stress relaxation data showed some similarities. All coatings displayed a rapid decrease in stress that occurred in the first 5–10 min as evidenced by a steep decline in the stress versus time plots. This is deemed stage I relaxation behavior. The second regime, deemed stage II, is described by a slower relaxation that extends to either full relaxation or the remaining

Table 2
Averaged modulus and applied strain values for the given coating condition at the test temperatures of 1100 °C and 1200 °C. The modulus values were determined from the slope of the loading curve by linear curve fit prior to stress relaxation at the listed temperature. The compliance of the load frame was accounted for in the measurement of E.

Coating condition	Test temp. (°C)	σ_o (MPa)	E (GPa)	Strain at σ_o	Number of samples
As-sprayed	1000	60	19 ± 3	0.0030 ± 0.0003	3
As-sprayed	1100	60	14 ± 4	0.0043 ± 0.0009	3
As-sprayed	1200	60	15 ± 3	0.0046 ± 0.0013	10
50 h/1000 °C	1100	60	20 ± 1	0.0033 ± 0.0008	2
50 h/1000 °C	1200	60	17 ± 6	0.0039 ± 0.0015	5
50 h/1200 °C	1100	60	20 ± 2	0.0031 ± 0.0002	2
50 h/1200 °C	1200	60	21 ± 1	0.0028 ± 0.0002	2

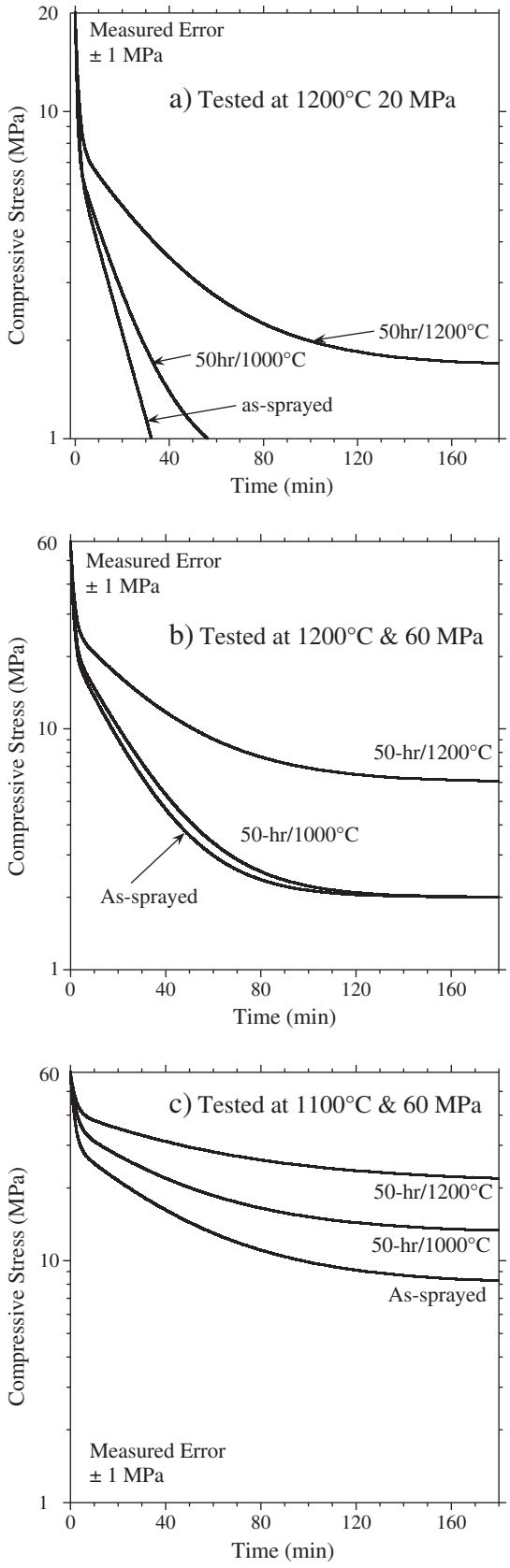

Fig. 1. The averaged stress relaxation response for varying stand-alone coating conditions tested at a) at the test temperature of 1200 °C under an initial 20 MPa compressive load, b) the test temperature of 1200 °C under an initial 60 MPa compressive load, and c) the test temperature of 1100 °C under an initial 60 MPa compressive load.

170 min of the test. As an example, the averaged stress relaxation behavior for three different coatings conditions, as-sprayed, heat treated for 50 h/1000 °C, and heat treated for 50 h/1200 °C prior to testing, are shown in Fig. 1a. The average curve fitting parameters for this sample are shown in Table 3. During stage I for the coating condition of 50 h/1000 °C relaxed at 1200 °C, for example, 64% of the initially applied 20 MPa is relaxed. Therefore, 13.8 MPa has been relaxed by the end of stage I, in a total time of $5\tau_1 = 5 * 57\ s = 285\ s$ or 4.8 min. Then during stage II, 32% of the initial 20 MPa is further relaxed, i.e. an additional 6.4 MPa is relaxed leaving only 0.8 MPa ($w_3 = 4\%$) un-relaxed in the coating. Thus, the 50 h/1000 °C condition relaxes 96% of σ_o, i.e. 19.2 MPa, in $5\tau_1 + 5\tau_2 = 5475\ s$ or 91 min. However, in the current study a coating is considered fully relaxed when the initial stress decays to 1 MPa, which as observed in Fig. 1, is achieved in only ≈3480 s or 58 min.

Of interest in the current study is delineating the effects of coating condition (including heat-treatment temperature and time), test temperature, and starting stress on the time constants of each Maxwell element. With a goal to limit stress relaxation in the coating during stage I or stage II relaxation, minimizing either w_1 or w_2, respectively, is desirable. For cases when the coatings are tending to the same w_1 or w_2, a higher τ_1 or τ_2, respectively, is desirable as it implies that relaxation will occur slower.

3.3. Effects of experimental variables on stage I relaxation

Test temperature strongly affected w_1. As-sprayed coatings stress tested at room temperature relax the applied stress. In fact, 8% of the initial 60 MPa stress is relaxed (see w_1 in Table 3) after $5\tau_1 = 5(39\ s) \approx 200\ s$. Furthermore, in the as-sprayed condition coatings relaxed 31%, 50%, and 65% of the starting 60 MPa for test temperatures of 1000 °C, 1100 °C, and 1200 °C. The stage I relaxation constant also decreased as test temperature increased, indicating faster relaxation of stress.

Heat-treatment of the coating prior to testing influenced stress relaxation; this was particularly true of the 1200 °C heat-treatment. For example, as-sprayed, 50 h/1000 °C and 50 h/1200 °C heat-treated coatings relaxed 50%, 40% and 32% of the starting 60 MPa stress during stage I relaxation for test conditions of 60 MPa/1100 °C. Despite these differences in stress relaxation behavior as a function of coating condition, a test temperature of 1200 °C generally had more effect on the thermomechanical behavior than prior coating heat-treatment. For example, it is interesting to note (see Table 3) that w_1 for any coating condition tested a 1200 °C and 20 or 60 MPa relaxed ~60% of the initial stress during Stage I relaxation.

Heat-treatment duration affected the amount of stress relaxed as shown in Table 4. For samples relaxed from 20 MPa at 1200 °C, w_1 decreased from 70% to 55% relaxed when the heat-treatment time was increased from 10 to 100 h, respectively. In contrast, the Stage I time constant was not a function of heat-treatment duration at 1200 °C. Lowering the test temperature from 1200 °C to 1100 °C for a coating heat-treated 50 h at 1200 °C decreased w_1 from 60% to 35% relaxed. There was also an increase in τ_1 from 78 to 95 s as a result of lowering the test temperature.

3.4. Effects of experimental variables on stage II relaxation

While stage I relaxation begins and ends rapidly, stage II relaxation occurs over a longer time frame. As-sprayed coatings tested at room temperature relaxed minimally ($w_2 \approx 6$–8%) in stage II. At the end of the 180 min test, w_3 values for as-sprayed coatings tested at room temperature supported 73% and 86% of the initially applied 20 and 60 MPa, respectively. In the as-sprayed condition coatings relaxed 26%, 37%, and 32% of the starting 60 MPa for test temperatures of 1000 °C, 1100 °C, and 1200 °C during stage II. The stage II relaxation constant also halved when the test temperature was increased from

Table 3
Average stress relaxation modeling values for coatings in the as-sprayed and heat-treated conditions as a function of test temperature, and initial applied stress.

Coating conditions		Test parameters		w_1 (%)	τ_1 (s)	w_2 (%)	τ_2 (s)	w_3 (%)	Replicate tests
HT temp. (°C)	HT time (h)	Test temp (°C)	σ_o (MPa)						
As-sprayed	0	25	20	19	19	8	1543	73	1
As-sprayed	0	25	60	8	39	6	2745	86	1
As-sprayed	0	1000	60	31 ± 2	125 ± 54	26 ± 3	2462 ± 603	43 ± 1	3
As-sprayed	0	1100	20	52 ± 3	102 ± 6	42 ± 6	2000 ± 250	6 ± 0	3
As-sprayed	0	1100	60	50 ± 2	95 ± 3	37 ± 2	2433 ± 126	13 ± 3	3
As-sprayed	0	1200	20	65 ± 0	62 ± 8	35 ± 0	1000 ± 265	0	3
As-sprayed	0	1200	60	65 ± 3	60 ± 9	32 ± 3	1217 ± 166	3 ± 2	3
1000	50	1100	60	40 ± 2	122 ± 1	38 ± 2	2563 ± 124	22 ± 0	2
1000	50	1200	20	64 ± 2	57 ± 11	32 ± 4	1038 ± 53	4 ± 2	2
1000	50	1200	60	64 ± 3	68 ± 6	33 ± 2	1342 ± 166	3 ± 2	3
1200	50	1100	20	35 ± 3	97 ± 6	30 ± 2	2967 ± 208	35 ± 5	3
1200	50	1100	60	32 ± 2	120 ± 12	33 ± 2	3500 ± 147	35 ± 2	3
1200	50	1200	20	60 ± 0	78 ± 3	31 ± 2	2008 ± 146	9 ± 2	3
1200	50	1200	60	57 ± 2	80 ± 10	33 ± 0	1925 ± 66	10 ± 3	3

1100 °C to 1200 °C, from ~2433 s to ~1217 s. As-sprayed coatings tested at 1000 °C retained ~43% of the 60 MPa after 3 h of testing, compared to ~13% and ~3% of 60 MPa after testing at 1100 °C and 1200 °C, respectively.

Coating condition has little effect on w_2 for samples tested at 1200 °C, with values of 33% σ_o noted for as-sprayed coatings and those heat treated for 50 h at 1000 °C or 1200 °C. However, heat-treatment does play a role in τ_2, effectively doubling it from 1000 s to 2000 s after a 50-hr heat-treatment at 1200 °C. It is worth noting that τ_2 is the same for the as-sprayed and 50 h/1000 °C heat treat conditions. Increasing the stress from 20 MPa to 60 MPa did not change the basic relaxation behavior as the curve fit parameters that describe relaxation behavior were essentially equivalent.

Heat treatments of 10, 50, or 100 h at 1200 °C had essentially no effect on w_2 for coatings tested at 1200 °C (Table 4). The stage II relaxation constant was ~2000 s for all 3 coating durations. However, coatings heat treated for 100 h at 1200 °C deformed less overall in the 3-hour test as evidenced by a higher percentage of stress still on the coating ($w_3 = 13\%$). Dropping the test temperature from 1200 °C to 1100 °C greatly reduced the deformation in the coating, with w_3 values of 30% noted.

3.5. Summary of Stress Relaxation Observations

As-sprayed coatings relax at room temperature, independent of any temperature-driven relaxation mechanisms. Stage I relaxation at 1100 °C or higher, as measured by w_1, accounts for at least 50% of the total stress relaxed despite occurring in only 5–10 min. For samples tested at 1200 °C, stage I relaxation accounts for 60–65% of the relaxation. The 1200 °C test temperature greatly influenced the percentage of relaxation in the coating, more so than the coating heat-treatment temperature. Prior coating heat-treatment did influence τ_2. As-sprayed coatings and those heat treated for 50 h at 1000 °C displayed similar relaxation behavior when stress relaxed at 1200 °C (see Fig. 1b) as compared to coatings previously heat treated at 1200 °C.

3.6. Strain-rate as a function of test temperature and coating condition

The effect of temperature on the strain rates for the as-sprayed coating condition is presented in Fig. 2a. Also apparent on the plot for each test temperature is the transition region between stage I and stage II deformation behavior. There is a clear difference in strain rate as the coating transitions between stage I and stage II behavior. Most of the data represented on the plot is from stage I, with rates of 10^{-6} through $10^{-7}\,s^{-1}$ represented. Stage II rates are much lower, nominally $10^{-8}\,s^{-1}$. As expected, the strain rates approach zero as stress tends to zero. For equivalent stress, as the test temperature was increased the strain rate was observed to be higher. The extracted strain rates appear to reasonably agree with the steady-state creep rates of 7 wt.% YSZ APS coatings over the temperatures of interest, which generally range between 10^{-6}–10^{-8} 1/s at applied stress 40–60 MPa [7,36].

The effects of heat-treatment on the strain rates of coatings during relaxation are presented in Fig. 2b for the test temperature of 1100 °C. Heat treatments resulted in lower strain rates at equivalent stresses.

4. Discussion

4.1. Room temperature deformation mechanisms contributing to stress relaxation

Room temperature stress relaxation experiments were conducted to isolate the effect of only microstructural features, independent of temperature, on mechanical response. As was shown in Table 3 as-sprayed coatings relax at room temperature. In a prior paper, Petorak [37] has suggested via a strain energy analysis that only a fraction of the coating material bears the initially applied load. Upon application

Table 4
Average stress relaxation modeling values for coatings in the heat-treated conditions as a function of test temperature, heat-treatment duration, and initial applied stress.

Coating conditions		Test parameters		w_1 (%)	τ_1 (s)	w_2 (%)	τ_2 (s)	w_3 (%)	Replicate tests
HT temp. (°C)	HT time (h)	Test temp (°C)	σ_o (MPa)						
1200	10	1100	20	35 ± 5	89 ± 8	37 ± 5	2850 ± 180	28 ± 3	3
1200	10	1100	60	32 ± 2	118 ± 26	36 ± 2	3412 ± 539	32 ± 0	3
1200	50	1100	20	35 ± 3	97 ± 6	30 ± 2	2967 ± 208	35 ± 5	3
1200	50	1100	60	32 ± 2	120 ± 12	33 ± 2	3500 ± 147	35 ± 2	3
1200	10	1200	20	70 ± 3	86 ± 14	25 ± 3	1933 ± 138	5 ± 0	3
1200	50	1200	20	60 ± 0	78 ± 3	31 ± 2	2008 ± 146	9 ± 2	3
1200	100	1200	20	55	85	32	1950	13	1

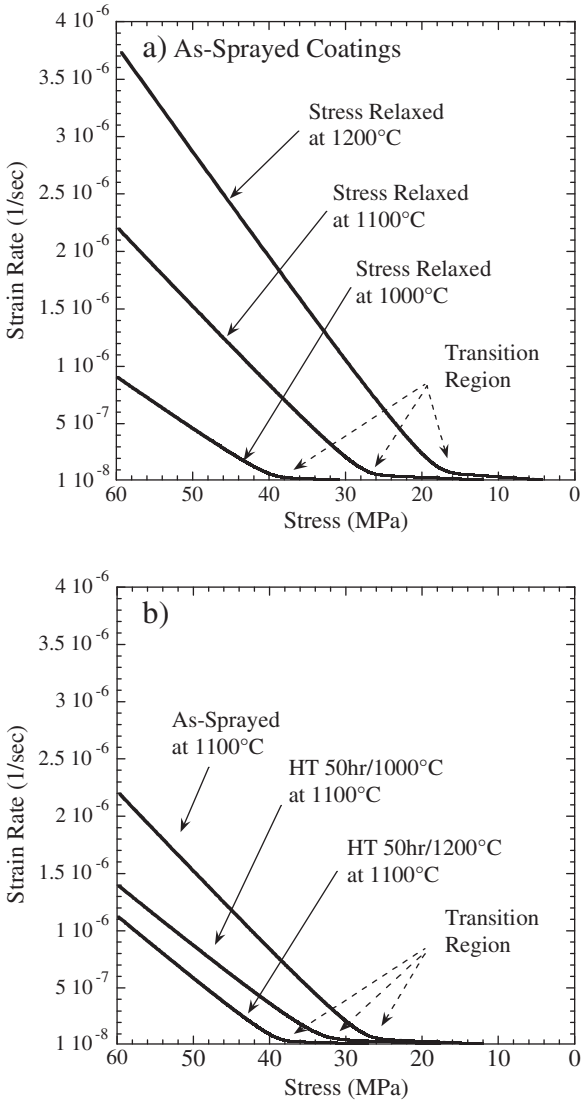

Fig. 2. (a) Strain rates of as-sprayed coatings extracted from stress relaxation experiments as a function of test temperature. Higher test temperatures result in larger strain rate values for equivalent stresses. Decreased stage I ranges, associated with smaller w_1 values, are indicated by the kink or bend in the curve occurring at larger stress values. (b) Strain rates extracted from stress relaxation experiments at 1100 °C as a function of coating condition. Heat treatments resulted in lower strain rates at equivalent stresses.

of stress, permanent deformation occurs in the sample as a result of void compaction and lamellae sliding, redistributing the load amongst a higher volume of the coating. Therefore, during the onset of stress relaxation there is a constant magnitude of strain induced on the sample, which is associated with a fraction of material bearing the load. The compaction of void systems and rearrangement of lamellae results in the release of stored elastic energy in the coating, while simultaneously more uniformly distributing the applied load [37]. Deformation mechanisms for Stage I behavior for tests conducted at elevated temperatures would include lamella sliding and compaction, as well as permanent closure of cracks oriented perpendicular to the applied stress as shown recently by Petorak et al [32].

4.2. High temperature deformation mechanisms contributing to stress relaxation

Service conditions in thermal barrier coatings are better represented by stress relaxation than creep. But, as shown in Fig. 2a and b, the stress relaxation data can be used to calculate an *instantaneous* strain rate as a function of stress at a given temperature. In turn, these extracted strain rate data can be compared to existing deformation mechanism maps (DMM) to help establish deformation mechanisms occurring during stress relaxation. From Fig. 2a and b there is clearly a transition in the strain rates from stage I to stage II relaxation. Stage I relaxation would correlate to the initial rapid increase in strain rate observed at the start of a creep test, i.e. primary creep. This data does not appear on DMMs as they are constructed from steady-state creep rates.

With consideration of stage II relaxation, YSZ has a melting temperature, T_m, of approximately 2700 °C according to binary phase diagram for ZrO_2–Y_2O_3 [38]. Operation at 1000°, 1100° and 1200 °C correlates to homologous temperatures, i.e. T/T_m, of 0.43, 0.46 and 0.50, respectively. The shear modulus for dense YSZ was calculated for each temperature based on the following equation [39]:

$$\mu = 93 - 0.021T \tag{7}$$

Where the shear modulus is in GPa and the temperature is in Kelvin. A normalized shear stress, based on the maximum initial compressive load of 60 MPa used during stress relaxation testing, was found to range from 10^{-3} to 10^{-4} between 1000° and 1200 °C. The coatings in the current study had columnar grains of approximately 0.1 to 1 μm in diameter, and 1–4 μm in height.

Inspection of a deformation mechanism map (DMM) for a 9.5 mol % cubic Y_2O_3–ZrO_2 (16.9 wt.% FSZ) with a grain size of 0.5 μm provided by Bowman [40] correlates the calculated normalized shear stress and homologous temperatures during stress relaxation to the Coble creep regime, where the dominant deformation mechanism is grain boundary diffusion. Diffusional data on 9.4 mol% Y_2O_3 fully stabilized cubic zirconia single crystals [41,42], and polycrystalline 16 mol% fully stabilized cubic zirconia [43,44] found oxygen to diffuse much faster than either cation, with the zirconium cation diffusing slightly slower than the yttrium cation [45], and therefore relaxation during stage II should be limited by the zirconium or yttrium cation diffusion. Through extensive creep testing on APS YSZ, Withey et al. [36] measured and also correlated deformation mechanisms, and the activation energies associated with them, to diffusional paths. These paths varied from surface diffusion of atoms at 1000 °C to bulk diffusion of atoms at 1200 °C.

DMM are generally constructed from dense materials. APS YSZ coatings are not dense, and the porous plasma-sprayed microstructure can accommodate a given amount of uniaxial strain through compaction of lamella and/or closure of pores. Hence, contributions to the strain rates can result from the compaction of lamella, which was established to occur in APS coatings through the room temperature experiments (see Table 3). In summary, the closure of void systems perpendicular to the applied load works in tandem with diffusional mechanisms during stress relaxation, where stage I (high strain rates) deformation is dominated by lamella compaction and crack closure (at higher temperatures), and stage II (lower strain rates) is dominated by diffusional creep mechanisms.

4.3. Temperature effects on the stress relaxation of plasma-sprayed stand-alone YSZ coatings

The effects of microstructural changes on stress relaxation behavior in plasma-sprayed coatings were elicited through pre-test heat-treatment of coatings at temperature known to either coarsen or densify microstructures in YSZ. Heat treatment of plasma-sprayed coatings at 1000 °C results in increased chemical bonding between lamellae splats, and smoothing of free surfaces, without reducing porosity. Heat treatment at 1200 °C reduces the volume of pores and cracks due to densification [18–22,33–35].

Coating heat treatments at 1000 °C prior to testing did behave differently than as-sprayed coatings when tested at 1100 °C; however,

these differences were no longer noted when the 50 h/1000 °C coatings were tested at 1200 °C. Thus, the spheroidization of microcracks to pores and microstructural coarsening appears to only have an effect when the temperature regime is below that where rapid densification can take place. Heat treatments at 1200 °C did strongly influence thermomechanical behavior at a test temperature of 1100 °C showing that the densified (as opposed to only coarsened) microstructure does influence stress relaxation (see Table 3). However, a test temperature of 1200 °C essentially nullified the 1200 °C heat-treatment effects with the exception of doubling the stage II relaxation constant. Clearly, this temperature in YSZ strongly influences thermomechanical behavior.

Stress relaxation at 1200 °C was chosen because it represents service temperatures in thermal barriers. As measured in the current study, coatings stress relaxed at 1200 °C demonstrated the greatest relaxation of the applied compressive stress. This is important because the greater the relaxation during service, the greater the tensile stress generated in the coating upon cooling. Stage I relaxation is responsible for much of the deformation that occurs in APS YSZ coatings. Table 3 indicated that stage I deformation of as-sprayed coatings at 1200 °C generally contributed to ≈66% of the overall deformation that occurred during the 180 min test, with most of that deformation occurring during the first 10 min. Thus, reduction of stage I deformation would be one strategy to reducing overall deformation in the coating system.

One approach to reduce stage I would be to heat treat the coating prior to service as the current study shows heat treatments at 1200 °C for times as short as 10 h (see Table 4) greatly reduced the stage I deformation in the coating. However, this is challenging to do because the coating is attached to the underlying superalloy. Upon heating the coating, the stiffer superalloy will constrain the coating, effectively putting the coating in compression. It is clear from this thought experiment that microstructural changes in the coating that would resist stage I deformation need to be incorporated into the coating while it is being applied, *not after its application* through a heat-treatment.

Microstructural changes that would reduce stage I deformation would include those that would sinter or chemically bond lamella, reducing their ability to slide or compact under applied stresses. With that in mind, it may be that "hotter" plasma spray conditions, generally controlled by the plasma composition, gun power or spray distance, would tend to chemically bond the lamella during application. This approach has been used in the development of plasma-sprayed coatings with vertical segmented cracks [46–48] and limited experimentation indicated reduced stress relaxation [49]. Another approach might be to infiltrate the pores with a medium that prevent compaction of the pores/cracks prior to placing the coating service. However, there will be a corresponding loss of necessary coating strain tolerance as the coating becomes stiffer. A balance would need to be achieved between the two competing effects.

Because stage II deformation is controlled by the intrinsic properties of the coating material, reducing it would likely require changing the composition of the material. Thus, creep data for coating materials that met requisite properties (temperature, environmental, processability, cost, etc.) should be considered with the goal of reducing steady-state creep rates at temperatures of 1200 °C or greater as compared to YSZ.

5. Conclusions

The stress relaxation behavior of APS YSZ thermal barrier coatings is a function of coating conditions and test temperature. A 1200 °C heat-treatment, for as short as 10 h, or a 1200 °C test temperature, most strongly influenced the coating behavior. Stage I relaxation is associated with the largest permanent reduction in stress, up to 65% in the as-sprayed case, and hence the most detrimental change with respect to recovery. Compaction and closure of cracks and pores, and the rearrangement and sliding of lamellae during stage I aid in relaxing applied compressive loads. Diffusional creep mechanisms likely contribute to the relaxation behavior of stage I but dominate during stage II. Stage II relaxation could be decreased by two methods, either decrease the porosity or utilize an oxide with slower diffusing species than Zr^{4+} or Y^{3+}. Microstructural design that would decrease stress relaxation in either stage I or stage II would require a careful balance of coating strain tolerance, compliance, and thermal conductivity.

Acknowledgement

Major portions of this research were funded by the National Science Foundation via grant DMR-0134286. Based in part on the thesis submitted by C. Petorak for the Ph.D. Degree in Materials Engineering, Purdue University, West Lafayette, Indiana, 2007.

References

[1] R.B. Heimann, Plasma Spraying Coating: Principles and Applications, Weinheim, New York, 1996.
[2] W. Beele, G. Marijnissen, A. van Lieshout, Surf. Coat. Technol. 120 (1999) 61.
[3] R.A. Miller, J. Therm. Spray Technol. 6 (1) (1997) 35.
[4] R.A. Miller, Surf. Coat. Technol. 30 (1) (1987) 1.
[5] K. Kokini, A. Banerjee, T.A. Taylor, Mater. Sci. Eng. A 323 (2002) 70.
[6] K. Kokini, Y.R. Takeuchi, B.D. Choules, Surf. Coat. Technol. 82 (1996) 77.
[7] G. Thurn, G.A. Schneider, F. Aldinger, Mater. Sci. Eng. A233 (1997) 176.
[8] G. Thurn, G.A. Schneider, F. Aldinger, Proceedings of the 2nd International Symposium on Thermal Stresses and Related Topics, 1997.
[9] R. Herzog, E. Trunova, R.W. Steinbrech, E. Wessel, R. VaBen, F. Schubert, L. Singheiser, International Conference on "Creep and Fracture in High Temperature Components-Design & Life Assessment Issues, Institution of Mechanical Engineers, Central London, UK, Sept 12-14, 2005.
[10] G.R. Dickinson, C. Petorak, K. Bowman, R. Trice, J. Am. Ceram. Soc. 88 (8) (2005) 2202.
[11] U. Messerschmidt, B. Baufeld, K.J. McClellan, A.H. Heuer, Acta Metall. Mater. 43 (5) (1995) 1917.
[12] A.H. Bartlett, R. Dal Maschio, J. Am. Ceram. Soc. 78 (4) (1995) 1018.
[13] L. Singheiser, R. Steinbrech, W.J. Quadakkers, R. Herzog, Mater. High Temp. 18 (4) (2001) 249.
[14] R. Herzog, P. Bednarz, E. Trunova, V. Shemet, R.W. Steinbrech, F. Schubert, Singheiser, L. Proceedings of the 30th International Conference and Exposition on Advanced Ceramics and Composites, Jan 22-27, American Ceramic Society, Cocoa Beach, FL, 2006.
[15] C. Petorak, J. Ilavsky, H. Wang, W. Porter, R. Trice, Surf. Coat. Tech. 205 (1) (2010) 57.
[16] S.R. Choi, D. Zhu, R.A. Miller, NASA/TM-2004-212625, National Aeronautics and Space Administration, Glenn Research Center, Cleveland, Ohio, 2004.
[17] D. Zhu, R.A. Miller, J. Therm. Spray Technol. 9 (2000) 175.
[18] D. Basu, C. Funke, R.W. Steinbrech, J. Mater. Res. Soc. 14 (12) (1999) 4643.
[19] B. Siebert, C. Funke, R. Vaben, D. Stover, J. Mater. Proces. Technol. 92–93 (1999) 217.
[20] H.E. Eaton, R.C. Novak, Surf. Coat. Technol. 32 (1987) 227.
[21] J.A. Thompson, T.W. Clyne, Acta Mater. 49 (2001) 1565.
[22] K. Erk, C. Deschaseaux, R. Trice, J. Am. Ceram. Soc. 89 (5) (2006) 1673.
[23] W.W. Mullins, J. Appl. Phys. 28 (3) (1957) 333.
[24] W.W. Mullins, AIME Trans. 218 (1960) 354.
[25] R.P. Ingel, D. Lewis III, J. Am. Ceram. Soc. 69 (4) (1986) 325.
[26] R.M. Christensen, Theory of Viscoelasticity – An Introduction, Academic Press, 1971.
[27] Y.C. Fung, Foundations of Solid Mechanics, Prentice-Hall, 1965.
[28] A.S. Krausz, H. Eyring, Deformation Kinetics, John Wiley & Sons, 1975.
[29] N.G. McCrum, C.P. Buckley, C.B. Bucknall, Principles of Polymer Engineering, 2nd EditionOxford Science Publications, 1997.
[30] A. Morales-Rodriquez, A. Bravo-Leon, M. Jimenez-Melendo, A. Domniguez-Rodriguez, J. Eur. Ceram. Soc. 22 (2002) 2641.
[31] E.W. Hart, H.D. Solomon, Acta Metall. 21 (March 1973) 295.
[32] C. Petorak, J. Ilavsky, H. Wang, W. Porter, R. Trice, Surf. Coat. Technol. 205 (2010) 57.
[33] J. Allen, J. Ilavksy, G.G. Long, J.S. Wallace, C.C. Berndt, H. Herman, Acta Mater. 49 (2001) 1661.
[34] J. Ilavsky, G.G. Long, A.J. Allen, C.C. Berndt, Mater. Sci. Eng. A272 (1999) 215.
[35] R.W. Trice, Y.J. Su, J.R. Mawdsley, K.T. Faber, A.R. De Arellano-López, H. Wang, W.D. Porter, J. Mater. Sci. 37 (2002) 2359.
[36] E. Withey, C. Petorak, R. Trice, G. Dickinson, T. Taylor, J. Eur. Ceram. Soc. 27 (16) (2007) 4675.
[37] C. Petorak, R.W. Trice, Journal of Coating and Surface Technology (in press).
[38] H.G. Scott, J. Mater. Sci. 10 (9) (1975) 1527.

[39] A. Dominguez-Rodriguez, K.P.D. Lagerlof, A.H. Heuer, J. Am. Ceram. Soc. 69 (3) (1986) 281.
[40] K. Bowman, Mechanical Behavior of Materials, John Wiley and Sons, Inc., New Jersey, 2004.
[41] H. Solomon, J. Chamat, C. Dolin, C. Monty, in: T.O. Mason, J.L. Routbort (Eds.), Ceramic Transactions, *Point Defects and Related Properties of Ceramics*, vol. 24, American Ceramic Society, Westerville, OH, 1991.
[42] F.R. Chien, A.H. Heuer, Philos. Mag. A 73 (3) (1996) 681.
[43] Y. Sakka, Y. Oishi, K. Ando, J. Mater. Sci. 17 (1982) 3101.
[44] Y. Oishi, K. Ando, Y. Sakka, in: M.F. Yang, A.H. Heuer (Eds.), *Advances in Ceramics*, *Additives and Interfaces in Electronic Ceramics*, 7, American Ceramic Society, Columbus, OH, 1983.
[45] M. Jimenez-Melendo, A. Dominguez-Rodriguez, A. Bravo-Leon, J. Am. Ceram. Soc. 81 (11) (1998) 2761.
[46] Thomas Taylor, Thermal Barrier Coatings for Substrates and Process for Producing It, US Patent 5073433 (1991).
[47] H.B. Guo, S. Kuroda, H. Murakami, J. Am. Ceram. Soc. 89 (4) (2006) 1432.
[48] R. Vassen, H.B. Guo, D. Stover, Adv. Ceram. Coat. Ceram. Met. Syst. Ceram. Eng. Sci. Proc. 26 (3) (2005) 37.
[49] M. Karger, R. Vassen, D. Stover, C. Petorak, R. Trice, International Thermal Spray Conference, 2008.